HHS Public Access

Author manuscript

J Biomol NMR. Author manuscript; available in PMC 2017 February 01.

Published in final edited form as:

J Biomol NMR. 2016 February ; 64(2): 143–151. doi:10.1007/s10858-016-0015-3.

Nitrogen-detected TROSY yields comparable sensitivity to proton-detected TROSY for non-deuterated, large proteins under physiological salt conditions

Koh Takeuchi[1,2], **Haribabu Arthanari**[3], **Misaki Imai**[4], **Gerhard Wagner**[3,*], and **Ichio Shimada**[1,5,*]

[1]Molecular Profiling Research Center for Drug Discovery, National Institute for Advanced Industrial Science and Technology, Tokyo 135-0063, Japan

[2]JST, PRESTO, Tokyo 135-0063, Japan

[3]Department of Biochemistry and Molecular Pharmacology, Harvard Medical School, Boston, MA 02115

[4]Research and Development Department, Japan Biological Informatics Consortium, Tokyo 135-0063, Japan

[5]Graduate Schools of Pharmaceutical Sciences, The University of Tokyo, Tokyo 113-0033, Japan

Abstract

Direct detection of the TROSY component of proton-attached ^{15}N nuclei (^{15}N-detected TROSY) yields high quality spectra with high field magnets, by taking advantage of the slow ^{15}N transverse relaxation. The slow transverse relaxation and narrow line width of the ^{15}N-detected TROSY resonances are expected to compensate for the inherently low ^{15}N sensitivity. However, the sensitivity of ^{15}N-detected TROSY in a previous report was one-order of magnitude lower than in the conventional ^{1}H-detected version. This could be due to the fact that the previous experiments were performed at low salt (0–50 mM), which is advantageous for ^{1}H-detected experiments. Here, we show that the sensitivity gap between ^{15}N and ^{1}H becomes marginal for a non-deuterated, large protein (τ_c = 35 ns) at a physiological salt concertation (200 mM). This effect is due to the high salt tolerance of the ^{15}N-detected TROSY. Together with the previously reported benefits of the ^{15}N-detected TROSY, our results provide further support for the significance of this experiment for structural studies of macromolecules when using high field magnets near and above 1 GHz.

Keywords

Nitrogen detection; TROSY; High field magnet; protein NMR; salt concentration; sensitivity

*Corresponding Authors: Gerhard Wagner: Department of Biochemistry and Molecular Pharmacology, Harvard Medical School, 240 Longwood Avenue, Boston, MA 02115, USA. Tel.: (617) 432 3213, Fax: (617) 432 4383, gerhard_wagner@hms.harvard.edu, Ichio Shimada: Graduate Schools of Pharmaceutical Sciences, The University of Tokyo, 7-3-1 Hongo, Bunkyo-ku, Tokyo 113-0033, Japan, shimada@iw-nmr.f.u-tokyo.ac.jp.

Introduction

Heteronuclear NMR experiments that directly detect resonances of nuclei with a low gyromagnetic ratio (γ), such as ^{13}C and ^{15}N, have recently been proposed to expand the utility of solution NMR in structural and functional studies of macromolecules (Takeuchi et al., 2012). A variety of experiments have been proposed for NMR analyses of proteins, using ^{13}C-direct detection (Arnesano et al., 2005; Bermel et al., 2003; Bermel et al., 2006a; Bermel et al., 2006b; Felli and Brutscher, 2009; Hsu et al., 2009; Lee et al., 2005; Serber et al., 2001; Takeuchi et al., 2010a; Takeuchi et al., 2008) and ^{15}N-direct detection (Gal et al., 2011; Levy and Richter, 1979; Takeuchi et al., 2015; Takeuchi et al., 2012; Takeuchi et al., 2010b; Vasos et al., 2006).

Recently, we reported that direct detection of the TROSY (Pervushin, 2000; Pervushin et al., 1997) component of ^{15}N (^{15}N-detected TROSY) is advantageous for maximizing the benefit of a low γ-nuclei detection experiment at a magnetic field higher than 14.1 T, which corresponds to 600 MHz in proton frequency (Takeuchi et al., 2015). Henceforth, we will use the frequency of the proton resonance for the description of field strength. We found that the ^{15}N-detected TROSY-HSQC spectrum of a protein with a 40 ns rotational correlation time (τ_c) can be recorded in a few hours, with additional resolution benefits. Unlike conventional ^{1}H-detected TROSY, uniform deuteration is not necessary for the ^{15}N-detected experiment. Thus, ^{15}N-detected TROSY provides a previously unexplored opportunity for NMR studies of proteins that can only be expressed in mammalian or insect cells, or proteins that cannot be refolded for amide back exchange after expression in D_2O media. Since ^{15}N-detected TROSY is expected to yield the narrowest NMR resonances, this method will help to resolve the signal degeneracy problems experienced with high molecular weight or unstructured systems.

Although the slow transverse relaxation and the narrow line width of the ^{15}N resonances are expected to compensate for the inherently low sensitivity of ^{15}N, the ^{15}N-detected TROSY still suffered from much lower sensitivity, as compared to the conventional ^{1}H-detected TROSY version (Takeuchi et al., 2015). However, it should be noted that the previous study was conducted under experimental conditions that are advantageous for the ^{1}H-detected experiments, including non-physiologically low salt concentrations (0–50 mM NaCl with less than 10 mM buffer). Here we show that, due to the significant tolerance of ^{15}N-detection under high-salt conditions, the disadvantage of ^{15}N-detected TROSY relative to ^{1}H-detected TROSY in terms of the sensitivity becomes marginal, for a small protein in high-salt (1 M) conditions. In addition, for a non-deuterated, large protein (τ_c = 35 ns), the sensitivities of ^{15}N- and ^{1}H-detected TROSY experiments become comparable at a physiological salt concentration (200 mM). These results indicate a wide applicability of the ^{15}N-detected TROSY for structural and functional studies of macromolecules under physiologically relevant conditions while not requiring sample deuteration.

Materials and methods

All chemicals were purchased from Sigma (St. Louis, MO) unless otherwise noted. All stable-isotope-labeled materials were acquired from Cambridge Isotope Laboratories (Cambridge, MA).

Expression and purification of the B domain of protein G (GB1)

The gene encoding His_6-tagged GB1, consisting of 64 amino acid residues, was cloned into the pET9d vector (Novagen, San Diego, CA) as previously described (Frueh et al., 2005). GB1 was expressed in commercially available BL21 (DE3) *E. coli* cells (Novagen) at 37 °C, and protein expression was induced for 6 h. For the uniformly $^{15}N^{13}C$ labeled samples, the cells were cultured in ^{15}N, ^{13}C M9 media containing 8.5 g/L Na_2HPO_4, 3 g/L KH_2PO_4, 0.5 g/L NaCl, 2mM $MgCl_2$, and 0.1 mM $CaCl_2$ in H_2O, which was supplemented with 3 g/L ^{13}C glucose and 1 g/L of $^{15}NH_4Cl$. The protein was purified by Ni-NTA affinity chromatography as previously described (Frueh et al., 2005).

Expression and purification of MBP

The 42-kDa maltose binding protein (MBP), which has been extensively studied in *E. coli* was used in this study (Gardner et al., 1998). MBP was expressed in commercially available BL21 (DE3) *E. coli* cells (Novagen) at 37 °C and protein expression was induced for overnight at the 30°C. To prepare the uniformly $^{15}N^{13}C$ labeled samples, the cells were cultured in ^{15}N, ^{13}C M9 media containing 8.5 g/L Na_2HPO_4, 3 g/L KH_2PO_4, 0.5 g/L NaCl, 2mM $MgCl_2$, and 0.1 mM $CaCl_2$ in H_2O, which was supplemented with 3 g/L ^{13}C glucose and 1 g/L of $^{15}NH_4Cl$. MBP was purified in a buffer containing 25 mM Tris–HCl (pH 7.6), 300 mM NaCl, and 1 mM EDTA, and was then loaded onto amylose resin (3 ml, New England Biolabs, Beverly, MA, USA), which was equilibrated with the buffer described above. After washing the resin, MBP was eluted with the same buffer supplemented with 10 mM maltose.

NMR Experiments

NMR spectra were recorded on a Bruker (Billerica, MA) Avance III 800 spectrometer equipped with a triple-resonance cryogenic probe with carbon/nitrogen at the inner coil and the cryogenic preamplifiers (TCXI) that are designed for heteronuclear-detection experiments. For our TCXI probe, the ^{15}N signal to noise ratio (SNR) for 90% formamide in DMSO-d6 is 138 against 2 ppm noise, which is slightly better than the manufacturer certified value for TCXI probes (SNR > 115). However, it should be noted that our TCXI probe shows unusual high sensitivity for ^{1}H detected experiments. The SNR for 0.1% ethyl benzene in $CDCl_3$ is 5800 against 200 Hz noise, which is more than two-fold greater than the manufacturer certified value for TCXI probes (SNR > 2300). The proton SNR value is almost comparable to the certified value for proton-optimized triple-resonance cryogenic probes with the proton inner coil and the cryogenic preamplifier (TCHI, SNR > 6000), which are designed for proton-detection experiments. Spectra of the uniformly labeled GB1 sample were recorded at 298 K, in a buffer containing 10 mM sodium phosphate (pH 6.8) and the indicated concentrations of NaCl. Spectra of the uniformly $^{15}N^{13}C$ labeled MBP sample were recorded at 283 K in buffer containing 10 mM HEPES-NaOH (pH 7.4), 1 mM

EDTA, and 2 mM β-cyclodextrin. The ^{15}N-detected and ^{1}H-detected TROSY-HSQC experiments performed here are the same as those reported previously (Takeuchi et al., 2015). The ^{15}N-detected TROSY-HSQC experiments were recorded with spectral widths of 40 ppm (^{15}N, direct) and 6 ppm (^{1}H, indirect). Acquisition times were set to 0.39 sec (^{15}N, direct dimension) and 0.013 sec (^{1}H, indirect dimension) for GB1. The ^{15}N-detected TROSY-HSQC experiments of GB1 were recorded for 2.1 hr at 800 MHz. Acquisition times were set to 0.31 sec (^{15}N, direct dimension) and 0.014 sec (^{1}H, indirect dimension) for MBP. The ^{15}N TRSOY-HSQC experiments of MBP were recorded for 8.5 hr at 800 MHz. The ^{1}H-detected TROSY-HSQC experiments were recorded so they had the same acquisition times for both the ^{15}N (indirect) and ^{1}H (direct) dimensions, as in the ^{15}N-detected experiments. The number of scans was set so that the ^{15}N-detected and ^{1}H-detected TROSY-HSQC have the same experimental time. The carbon decoupling was achieved by using a p5m4 supercycle (Fujiwara and Nagayama, 1988), with an adiabatic CHIRP pulse of 2.5 ms length and 25% smoothing (Bohlen and Bodenhausen, 1993). Zero filling was applied for each FID, but no apodization function was used for the direct dimension before Fourier transformation. For the indirect dimensions, zero filling and a cosine-apodization function were applied. The recycling delay was set to 1.0 s, for both the ^{15}N-detected and ^{1}H-detected TROSY-HSQC experiments. The tuning, matching, and 90° hard pulses were optimized for all of the ^{1}H, ^{13}C, and ^{15}N channels without any problems under all conditions reported here. All spectra were processed with TOPSPIN (Bruker; Billerica, MA) and analyzed with the program Sparky (Goddard and Kneller).

Calculation of transverse relaxation rates

The transverse relaxations of the decoupled spin I (R_{2I}) were calculated based on the standard expression, as follows:

$$R_{2I}=\sum_j^n p_{IS_j}^2 \left[(4J(0)+3(J(\omega_I)+J\left(|\omega_I-\omega_{S_j}|\right)+6J(\omega_I)+6J\left(\omega_I+\omega_{S_j}\right)\right]+\delta_I^2[(4J(0)+3(J(\omega_I)] \quad (1)$$

$$p_{IS_j}=-(\frac{\mu_0}{2\sqrt{2}})\frac{\gamma_I\gamma_{S_j}\hbar}{r_{IS_j}^3} \quad (2)$$

$$\delta_I=-(\frac{\mu_0}{3\sqrt{2}})\gamma_I B_0\Delta\sigma_I, \quad (3)$$

where $\Delta\sigma_I$ is the difference between the axial and the perpendicular principal components of the axially symmetric chemical shift tensors. The spectrum density was estimated using equation (4)

$$J(\omega)=2\tau_c/(5\times(1+(\tau_c\omega)^2), \quad (4)$$

where ω is the Larmor frequencies of the ^{1}H and ^{15}N spins, or their sum or difference.

The TROSY (R_{2I_T}) and anti-TROSY ($R_{2I_{AT}}$) transverse relaxations of spin I were calculated, as follows:

$$R_{2I_T} = R_{2I} - |Cp_{IS}\delta_I[4J(0)]| \quad (5)$$

$$R_{2I_{AT}} = R_{2I} + |Cp_{IS}\delta_I[4J(0)]| \quad (6)$$

$$C = (3\cos^2\Theta - 1), \quad (7)$$

where Θ is the angle between the unique tensor axes of the dipole-dipole interactions and the chemical shift anisotropies (CSA) interaction. For the calculation of the transverse relaxation rates, the dipole-dipole interactions with directly bonded nuclei, as well as nuclei within defined distances, and the chemical shift anisotropies were taken into consideration, to mimic the typical proton density in a protein. For the estimation of the dipole-dipole interactions in a uniformly ^{15}N-labeled protein, the typical distances in the α-helix region were used with the following distance cut-off criteria: < 4.5 Å for ^{1}H-^{1}H pairs and < 2.1 Å for ^{1}H-^{15}N pairs. These are the sequential H_{Ni}-H_{Ni+1} distance (2.8 Å), H_{Ni}-H_{Ni+2} distance (4.2 Å), intra residue H_{Ni}-$H\alpha_i$ distance (2.2 Å), sequential H_{Ni}-$H\alpha_{i+1}$ distance (3.5 Å), H_{Ni}-$H\alpha_{i+2}$ distance (4.4 Å), H_{Ni}-$H\alpha_{i+3}$ distance (3.4 Å), H_{Ni}-$H\alpha_{i+3}$ distance (4.2 Å), intra residue H_{Ni}-$H\beta_i$ distance (2.5 Å), and sequential H_{Ni}-$H\beta_{i+1}$ distance (3.0 Å) for proton pairs. Contributions from remote protons that are more than 4 residues away in a.a. sequences are not considered. As for the estimation of the dipole-dipole interactions in a uniformly ^{2}H^{15}N-labeled protein, the same nuclei that were considered in the case of a uniformly ^{1}H^{15}N-labeled protein were used, while all non-exchangeable protons were replaced with deuterium. CSAs were also included in the calculation ($\Delta\sigma^{15}N_H$: −160ppm, $\Delta\sigma^1H_N$: 16 ppm). The angle between the unique tensor axes of the dipole-dipole interactions and the CSA interaction (Θ) was set to 17° for $^{15}N_H$.

Results and discussion

Salt concentration dependence of ^{15}N-detected and ^{1}H-detected TROSY resonances

The sensitivity factor, L, of a cyrogenic probe can be expressed as

$$L = \left(1 + 7.45\frac{R_s}{R_c}\right)^{-0.5} \quad (8)$$

$$R_s = \frac{\pi\omega^2\mu^2\sigma n^2 b^4 l}{32(a^2 + (l/2)^2)}, \quad (9)$$

where Rs, Rc, a, b, l, n, μ, ω, and σ are the resistance of the sample, the resistance of the coil, the coil radius, the sample radius, the sample length, the number of coil turns, the permeability of free space, the Larmor frequency, and the sample conductivity, respectively (Kelly et al., 2002). Based on the relation, it has been shown that the effect of high ionic

conductivity on the ^{13}C-detecetd experiments is milder, as compared to that on the ^{1}H-detected experiments (Shimba et al., 2004). Since the Larmor frequency of ^{15}N is about one-tenth of that of ^{1}H, the loss of sensitivities due to high ionic conductivity is expected to be even less in the ^{15}N-detected experiments, as compared to both the ^{1}H- and ^{13}C-detected experiments. In theory, increasing the NaCl concentration from 0 mM to 200 mM would reduce the sensitivity of the ^{1}H-detected experiment to less than 50%. However, the ^{15}N-detected experiment is much less susceptive to the increase in salt concentration, and thus the sensitivity reduction induced by 200 mM NaCl is expected to be only about 5%. In addition to the reduction in sensitivity originating from the lower detection efficiency, the inhomogeneous excitation of nuclei in a sample would negatively affect the resultant sensitivity of the experiments. This effect is also much less detrimental in the ^{15}N-detected experiment. The inhomogeneous excitation would also cause insufficient solvent suppression, but would only affect the ^{1}H-detected experiment.

In order to experimentally confirm the effect of the salt concentration on the ^{15}N-detected (Takeuchi et al., 2015) and ^{1}H-detected (Pervushin, 2000; Pervushin et al., 1997) TROSY-HSQC experiments, the fixed concentration (1 mM) of uniformly ^{15}N^{13}C-labeled GB1 was dissolved in buffer with different salt concentrations, ranging from 10 mM to 1 M. All spectra were recorded with a triple-resonance cryogenic TCXI probe with cryogenic preamps and the inner coil for ^{15}N and ^{13}C, which are designed for heteronuclear-detection experiments. The salt concentration dependency of the resonances in the ^{15}N-detected and ^{1}H-detected TROSY-HSQC experiments is shown in Figure 1A and 1B. With the increase in NaCl concentration, the signal height of the ^{1}H-detected resonances was reduced significantly, and the signal height was less than 25% with 1 M NaCl, as compared to the 10 mM NaCl condition (Figure 1C; red). In contrast, the signal height of the ^{15}N-detected resonances was substantially less affected, even at a 1 M salt concentration (Figure 1C; blue). The signal reduction was only about 20% with 1 M NaCl, as compared to 10 mM NaCl. The signal reduction was slightly more than expected, however, this was mainly due to the inhomogeneous excitation and inversion of the ^{1}H nuclei in the single transition-to-single transition polarization transfer (ST^{2}PT) coherence transfer. In Figure 1D and 1E, the 2D ^{15}N-detected and ^{1}H-detected TROSY-HSQC experiments are compared under 1 M NaCl conditions. As shown in the figure, the disadvantage of the ^{15}N-detected TROSY-HSQC experiment relative to the ^{1}H-detected TROSY-HSQC experiment, in terms of the sensitivity, becomes marginal for this small protein (MW: 8K) under the high-salt conditions.

If one assumes identical noise, efficiency in signal detection, and no B_0/B_1 field inhomogeneity, then the relative intensity (or peak area after FT) of the ^{1}H-excited ^{15}N-detected experiments (^{15}N-detected TROSY-HSQC), as compared to that of the ^{1}H-excited ^{1}H-detected experiments (^{1}H-detected TROSY-HSQC) becomes 0.032. Therefore, the marginal difference in the sensitivity of the ^{15}N-detected TROSY-HSQC experiment relative to the ^{1}H-detected TROSY-HSQC experiment under high salt conditions clearly indicates that the ^{15}N-detection had an additional benefit, in that it avoided the detrimental effects of the high salt concentration on the sensitivity factor defined by the electric/thermal noise levels and the influence of the B_0/B_1 field inhomogeneity.

Management of ^{2}J and ^{3}J scalar couplings in ^{15}N-detected TROSY-HSQC

It should also be noted that the experiments were performed with non-deuterated GB1. Since the ^{15}N-detected TROSY-HSQC experiment should be recorded without broad-band ^{1}H decoupling in the detection period, the ^{15}N-detected resonances are broadened (or split) due to the ^{2}J and ^{3}J coupling to Hα and Hβ, respectively, and their signal heights were reduced (Figure 2A). The ^{2}J and ^{3}J scalar coupling can be removed by the application of a proton composite decoupling that is selective to the aliphatic proton resonances in the ^{15}N-detection period (Figure 2B). As shown in Figure 2C, the broadening (or splitting) of several resonances was significantly reduced and the signal heights become higher with the application of the selective ^{1}H decoupling. Thus, the difference in the sensitivity between the ^{15}N-detected and ^{1}H-detected resonances would be even smaller with the removal of the ^{2}J and ^{3}J couplings. However, in most cases, the improvements in the signal height were not significant, as expected from the reduction of the line width. This appears to be due to the small sideband of the selective decoupling pulses, which affects the H_N resonance. This effect causes the mixing of the sharp TROSY and the broad anti-TROSY coherences. Since the anti-TROSY resonances are expected to be 10-times broader, as compared to the TROSY resonances, even 1% of the mixing by the aliphatic proton decoupling would reduce the intensity of the TROSY resonances by 10%.

Sensitivity of ^{15}N-detected TROSY for a non-deuterated, large protein under physiological salt conditions

Figure 3 shows a comparison of the calculated transverse relaxation rates (R_2) for the ^{15}N-detected and ^{1}H-detected TROSY experiments, for deuterated and non-deuterated proteins at 800 MHz. In a deuterated system, R_2 of ^{15}N-detected TROSY is 3-fold less, as compared to that of ^{1}H-detected TROSY. However, the difference in R_2 becomes much more substantial under non-deuterated conditions, and the R_2 of ^{15}N-detected TROSY is 10-fold slower than that of ^{1}H-detected TROSY. As a result, the coherences loss during the pulse schemes are much less substantial for ^{15}N-detected TROSY-HSQC, as compared to those for ^{1}H-detected TROSY-HSQC, for a non-deuterated, large protein. Therefore, the disadvantage in the sensitivity of the ^{15}N-detected TROSY-HSQC experiment relative to the ^{1}H-detected TROSY-HSQC experiment would largely be resolved, for a non-deuterated, large protein at a physiological salt concentration.

Figure 4 shows the ^{15}N-detected TROSY-HSQC spectra (left) and the ^{1}H-detected TROSY-HSQC spectra (right) of non-deuterated maltose binding protein (0.5 mM) in complex with 2 mM β-cyclodextrin, dissolved in 10 mM HEPES-NaOH buffer (pH 7.4) with 200 mM NaCl. Both spectra were recorded in 8.5 h at 283K, and the apparent τ_c of the system is 35 ns. All of the resonances that were observed in the ^{1}H-detected TROSY-HSQC spectrum were also observed in the ^{15}N-detected TROSY-HSQC spectrum, with the exception of the arginine side chains, which are folded in the indirect dimension of the ^{1}H-detected spectrum but outside the spectrum width of the direct dimension in the ^{15}N-detected spectrum, and the asparagine and glutamine sidechain resonances that are not efficiently refocused in the ^{15}N-detected spectrum. As the result, only the mainchain resonances and tryptophan sidechain resonances are observed in the ^{15}N-detected TROSY-HSQC spectrum, and the signal heights of the resonances varied less relative to each other. Furthermore, the results clearly indicated

that the heights or the signal to noise ratios of the resonances from the structured region (shadowed) of the ^{15}N-detected TROSY-HSQC experiment are now comparable to those of the ^{1}H-detected TROSY-HSQC spectrum, and the sensitivity difference between these two experiments is now less than two-fold.

Due to the significant tolerance of the ^{15}N-detected TROSY-HSQC experiment to high salt conditions and with the benefit of the ^{15}N-detected TROSY-HSQC under non-deuterated conditions, the sensitivity difference between the ^{15}N-detected and ^{1}H-detected experiments becomes marginal for a small protein in a buffer with 1M NaCl and a non-deuterated, large protein at a physiological salt concentration (200 mM NaCl). These results further assure the significance of the ^{15}N-detected TROSY in exploitations of the high resolution and sensitivity offered by high field magnets above 1 GHz, as expected from the previous estimation (Takeuchi et al., 2015). It should be noted that the sensitivity for the ^{1}H-detected experiments would be higher with a triple-resonance TCHI cryogenic probe with the proton inner coil and the cryogenic preamps under low salt conditions. However, for samples with physiological salt concentrations, there is no significant difference in the ^{1}H sensitivity between the TCXI and TCHI probes.

The ^{1}H sensitivity under high salt conditions can be improved by using shaped or smaller diameter tubes. For example, in the TCHI probes, the SNR per unit volume has reportedly been improved by 2.2-fold for a ^{1}H-detected experiment by using the slot tube, as compared to the 5 mm round tube (Takeda et al., 2011). Thus, for ^{1}H-detected experiments, the shaped or smaller diameter tubes would provide better sensitivity, especially for proteins that can be concentrated into a smaller volume without aggregation or precipitation. However, for proteins with limited solubility, the advantage of the using those tubes would be limited and may be worse for small diameter tubes (Takeda et al., 2011). It should also be noted that the sensitivity gain of the ^{1}H-detected experiment with these tubes may actually be smaller than the reported value with the TCXI probes, since the ^{1}H coil is farther away, as compared to the TCHI probes. Note that, due to the ongoing developments in hardware, the relative sensitivity of the ^{15}N-detected experiments, as compared to the ^{1}H-detected experiments, may vary depending on the different generations of the probe systems. Nevertheless, the higher resolutions and the dispensable deuteration remain as the clear advantages of the ^{15}N-detected experiments over the ^{1}H-detected experiments.

Although a lower concentration of salt (< 100 mM) is usually recommended for ^{1}H-detected experiments, certain amounts of salts, including buffers etc, are often required to obtain a sample with a sufficient protein concentration for structural studies (Bagby et al., 2001; Golovanov et al., 2004). In addition, certain applications, such as residual dipole coupling measurements, structural analyses of membrane proteins in ionic detergents, and protein unfolding studies, require increased concentrations of salt and/or ionic materials, in order to perform the experiments under optimal conditions. Indeed, salt concentrations above 200 mM were used in 8 out of 46 cases (17%) in reports published in volume 9, issue 2 of Biomolecular NMR Assignment in 2015, and the average ± standard deviations of the ionic strength were 164 ± 116 mM. In addition, in 10 out of 46 cases (22%), the ionic strength was higher than that used for the MBP sample in this manuscript (218 mM). It should be noted that the conductivity of a sample is not only defined by the ionic strength but by the

mobility in solution (Kelly et al., 2002), and the statistics clearly indicates that high ionic conditions are required in many cases. Furthermore, the susceptibility of ^{1}H-detected experiments to salt is expected to be more severe at higher fields, where ^{15}N-detected TROSY would have maximal benefits in resolution and sensitivity.

Since the relaxation of ^{15}N TROSY is slower than that of ^{1}H TROSY, the ^{15}N-detection has the benefit that a longer acquisition in the indirect ^{15}N dimension is avoided as would be needed in the ^{1}H-detected experiment. This benefit is compounded by the use of a smaller spectral width (~6 ppm) in the indirect ^{1}H dimension centered at the amide resonances. As a consequence, the chemical shift sampling of the indirect ^{1}H dimension becomes more efficient in the ^{15}N-detected experiment, and the number of scans per increment in a given total experimental time can be increased. These benefits would also contribute to closing the sensitivity gap of the ^{15}N-detected TROSY-HSQC experiment, relative to that of the ^{1}H-detected experiment. In addition, although the dispersion in the ^{15}N dimension is almost invariant, the ^{1}H dispersion is wider for structured proteins but is narrower for intrinsically disordered proteins (IDPs), and thus the sampling in the indirect dimension becomes even more efficient for this class of proteins.

Supplementary Material

Refer to Web version on PubMed Central for supplementary material.

Acknowledgments

This work was supported by METI (Grant name: development of core technologies for innovative drug development based upon IT) to IS and by NIH grants GM047467 and AI 37581 to GW. This work was also partly supported by JST, PRESTO to KT. Maintenance of NMR instruments was supported in part by NIH grant EB002026.

References

Arnesano F, Banci L, Piccioli M. NMR structures of paramagnetic metalloproteins. Q Rev Biophys. 2005; 38:167–219. [PubMed: 16674835]

Bagby, S.; Tong, KI.; Ikura, M. [2] - Optimization of Protein Solubility and Stability for Protein Nuclear Magnetic Resonance. In: James, Thomas VDaUSL., editor. Methods in Enzymology. Academic Press; 2001. p. 20-41.

Bermel W, Bertini I, Felli IC, Kummerle R, Pierattelli R. ^{13}C Direct detection experiments on the paramagnetic oxidized monomeric copper, zinc superoxide dismutase. J Am Chem Soc. 2003; 125:16423–16429. [PubMed: 14692785]

Bermel W, Bertini I, Felli IC, Lee YM, Luchinat C, Pierattelli R. Protonless NMR experiments for sequence-specific assignment of backbone nuclei in unfolded proteins. J Am Chem Soc. 2006a; 128:3918–3919. [PubMed: 16551093]

Bermel W, Bertini I, Felli IC, Piccioli M, Pierattelli R. ^{13}C-detected protonless NMR spectroscopy of proteins in solution. Prog Nucl Magn Res Spec. 2006b; 48:25–45.

Bohlen JM, Bodenhausen G. Experimental Aspects of Chirp NMR Spectroscopy. Journal of Magnetic Resonance, Series A. 1993; 102:293–301.

Felli I, Brutscher B. Recent advances in solution NMR: fast methods and heteronuclear direct detection. ChemPhysChem. 2009; 10:1356–1368. [PubMed: 19462391]

Frueh DP, Arthanari H, Wagner G. Unambiguous assignment of NMR protein backbone signals with a time-shared triple-resonance experiment. J Biomol NMR. 2005; 33:187–196. [PubMed: 16331423]

Fujiwara T, Nagayama K. Composite inversion pulses with frequency switching and their application to broadband decoupling. Journal of Magnetic Resonance (1969). 1988; 77:53–63.

Gal M, Edmonds KA, Milbradt AG, Takeuchi K, Wagner G. Speeding up direct (15)N detection: hCaN 2D NMR experiment. J Biomol NMR. 2011; 51:497–504. [PubMed: 22038648]

Gardner KH, Zhang X, Gehring K, Kay LE. Solution NMR Studies of a 42 KDa Escherichia Coli Maltose Binding Protein/β-Cyclodextrin Complex: Chemical Shift Assignments and Analysis. Journal of the American Chemical Society. 1998; 120:11738–11748.

Goddard, TD.; Kneller, DG. SPARKY. Vol. 3. University of California; San Francisco:

Golovanov AP, Hautbergue GM, Wilson SA, Lian LY. A Simple Method for Improving Protein Solubility and Long-Term Stability. Journal of the American Chemical Society. 2004; 126:8933–8939. [PubMed: 15264823]

Hsu STD, Bertoncini CW, Dobson CM. Use of protonless NMR spectroscopy to alleviate the loss of information resulting from exchange-broadening. J Am Chem Soc. 2009; 131:7222–7223. [PubMed: 19432443]

Kelly AE, Ou HD, Withers R, Dötsch V. Low-Conductivity Buffers for High-Sensitivity NMR Measurements. Journal of the American Chemical Society. 2002; 124:12013–12019. [PubMed: 12358548]

Kupce Ē, Freeman R. Optimized Adiabatic Pulses for Wideband Spin Inversion. Journal of Magnetic Resonance, Series A. 1996; 118:299–303.

Lee D, Hilty C, Wider G, Wüthrich K. Effective rotational correlation times of proteins from NMR relaxation interference. J Magn Reson. 2006; 178:72–76. [PubMed: 16188473]

Lee D, Vögeli B, Pervushin K. Detection of C',C^{α} correlations in proteins using a new time- and sensitivity-optimal experiment. J Biomol NMR. 2005; 31:273–278. [PubMed: 15928994]

Levitt MH, Freeman R. Composite pulse decoupling. Journal of Magnetic Resonance (1969). 1981; 43:502–507.

Levy, G.; Richter, R. Nitrogen 15 Nuclear Magnetic Resonance Spectroscopy. John Wiley & Sons; 1979.

Pervushin K. Impact of transverse relaxation optimized spectroscopy (TROSY) on NMR as a technique in structural biology. Q Rev Biophys. 2000; 33:161–197. [PubMed: 11131563]

Pervushin K, Riek R, Wider G, Wuthrich K. Attenuated T2 relaxation by mutual cancellation of dipole-dipole coupling and chemical shift anisotropy indicates an avenue to NMR structures of very large biological macromolecules in solution. Proc Natl Acad Sci U S A. 1997; 94:12366–12371. [PubMed: 9356455]

Serber Z, Richter C, Dotsch V. Carbon-detected NMR experiments to investigate structure and dynamics of biological macromolecules. Chembiochem. 2001; 2:247–251. [PubMed: 11828451]

Shimba N, Kovacs H, Stern AS, Nomura AM, Shimada I, Hoch JC, Craik CS, Dötsch V. Optimization of ^{13}C direct detection NMR methods. J Biomol NMR. 2004; 30:175–179. [PubMed: 15557804]

Takeda M, Hallenga K, Shigezane M, Waelchli M, Löhr F, Markley JL, Kainosho M. Construction and performance of an NMR tube with a sample cavity formed within magnetic susceptibility-matched glass. J Magn Reson. 2011; 209:167–173. [PubMed: 21316281]

Takeuchi K, Arthanari H, Shimada I, Wagner G. Nitrogen detected TROSY at high field yields high resolution and sensitivity for protein NMR. J Biomol NMR. 2015

Takeuchi K, Frueh DP, Hyberts SG, Sun ZJ, Wagner G. High-resolution 3D CANCA NMR experiments for complete mainchain assignments using C_a direct-detection. J Am Chem Soc. 2010a in press.

Takeuchi K, Gal M, Shimada I, Wagner G. Low γ-nuclei detection experiments for bimolecular NMR. Recent Developments in Biomolecular NMR. 2012:25–52.

Takeuchi K, Heffron G, Sun ZY, Frueh DP, Wagner G. Nitrogen-detected CAN and CON experiments as alternative experiments for main chain NMR resonance assignments. J Biomol NMR. 2010b; 47:271–282. [PubMed: 20556482]

Takeuchi K, Sun ZY, Wagner G. Alternate ^{13}C-^{12}C labeling for complete mainchain resonance assignments using C^a direct-detection with applicability toward fast relaxing protein systems. J Am Chem Soc. 2008; 130:17210–17211. [PubMed: 19049287]

Vasos PR, Hall JB, Kummerle R, Fushman D. Measurement of 15N relaxation in deuterated amide groups in proteins using direct nitrogen detection. J Biomol NMR. 2006; 36:27–36. [PubMed: 16967194]

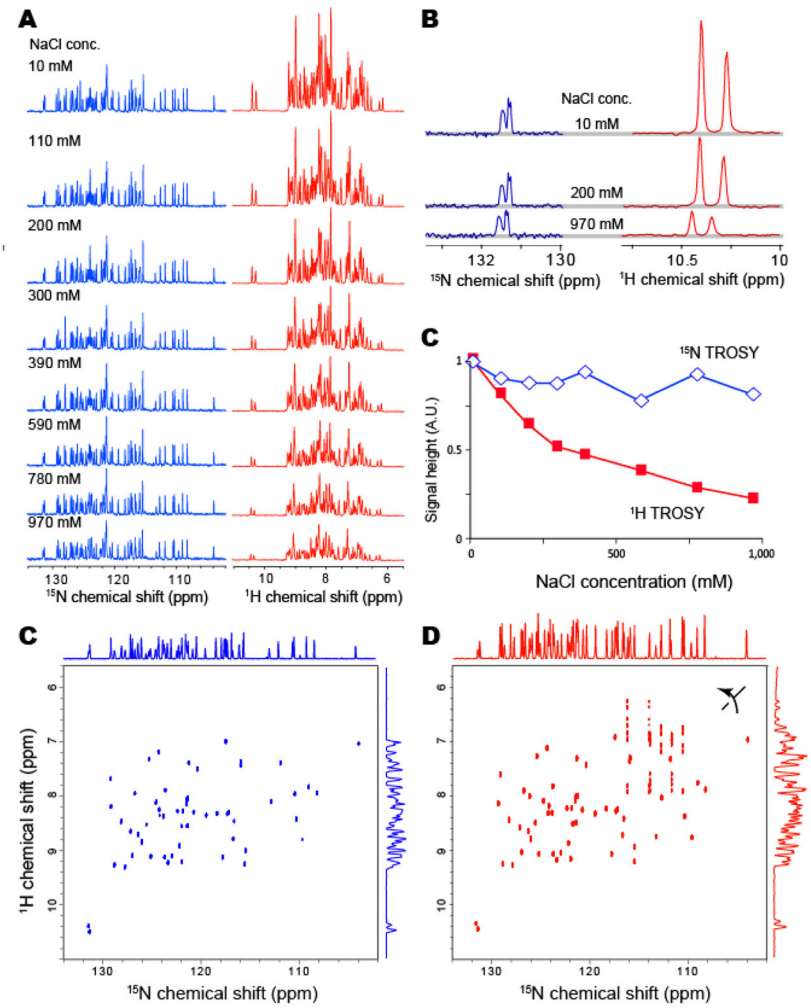

Figure 1. Salt concentration dependence of ^{15}N-detected and ^{1}H-detected TROSY resonances

(A) Salt concentration dependence of one-dimensional ^{15}N-detected (left) and ^{1}H-detected (right) TROSY resonances of GB1 with indicated concentrations of NaCl. (B) Selected enlarged views of (A). The concentration of U-^{15}N^{13}C GB1 was 1 mM, and the protein was dissolved in 10 mM phosphate buffer (pH 6.8). The spectra were recorded at 298K and 800 MHz. (B) Salt concentration dependence of the signal height of the lower-field resonance in (A). (C and D) The two-dimensional (C) ^{15}N-detected and (D) ^{1}H-detected TROSY-HSQC spectra of U-^{15}N^{13}C GB1, in 10 mM phosphate buffer (pH 6.8) with 1 M NaCl. The spectra was recorded at 298K at 800 MHz.

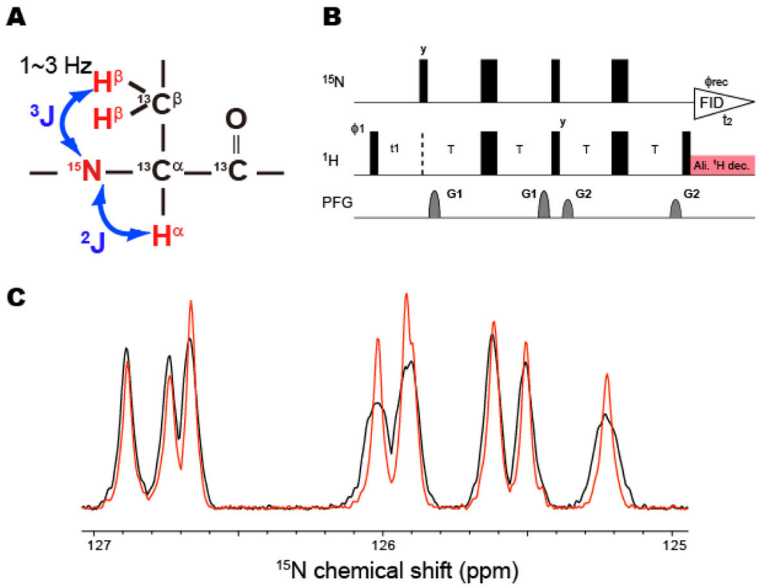

Figure 2. Application of selective composite decoupling to aliphatic proton resonances in the ^{15}N-detected TROSY-HSQC experiment

(A) The ^{2}J and ^{3}J couplings to Hα and Hβ, which cause the broadening (splitting) of the ^{15}N-detected TROSY resonances. (B) The modified pulse sequence of the ^{15}N-detected 2D TROSY-HSQC experiments. Narrow and wide rectangular black bars indicate non-selective π/2 and π pulses, respectively. All pulses were applied along the x-axis unless otherwise indicated. The delay T was set to 2.7 ms. The phase cycle employed was φ_1 = (y -y x –x), and φ_{rec} = (x -x -y y). Phase sensitive spectra in the indirect ^{1}H dimension (t_1) were obtained by incrementing the phase φ_1. The recycling delay was set to 1 s. The two sine-shaped pulsed field gradients were applied along the z-axis for 1.0 ms, with maximum intensities of G1 = 22.5 G/cm and G2 = 25 G/cm. The selective aliphatic decoupling was achieved by 0.1 kHz constant-adiabaticity WURST decoupling pulses centered at 1 ppm with a 4 kHz band width (Kupce and Freeman, 1996), which were applied in an MLEV manner (Levitt and Freeman, 1981). (C) One-dimensional ^{15}N-detected TROSY resonances of U-^{15}N^{13}C GB1 with (red) and without (black) aliphatic proton selective composite decoupling. The spectra were recorded at 283K, in 10 mM phosphate buffer with 100 mM NaCl.

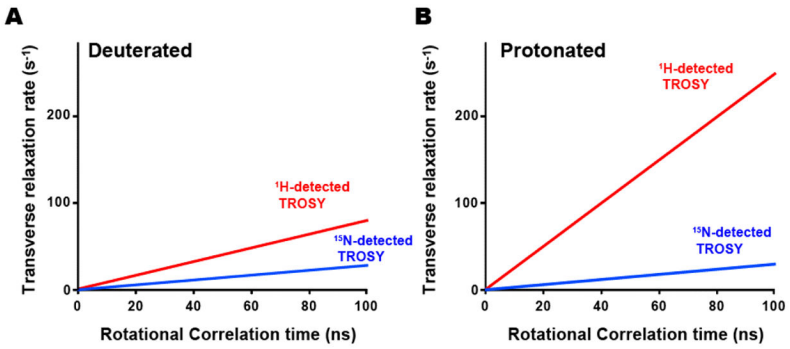

Figure 3. Transverse relaxation rates of the ^{15}N-detected (blue) and ^{1}H-detected (red) TROSY resonances for a (A) deuterated and (B) non-deuterated protein, as a function of the rotational correlation time

The transverse relaxation rates were calculated based on equation (5) in the supplemental materials and methods. The magnetic field strength was set to 800 MHz.

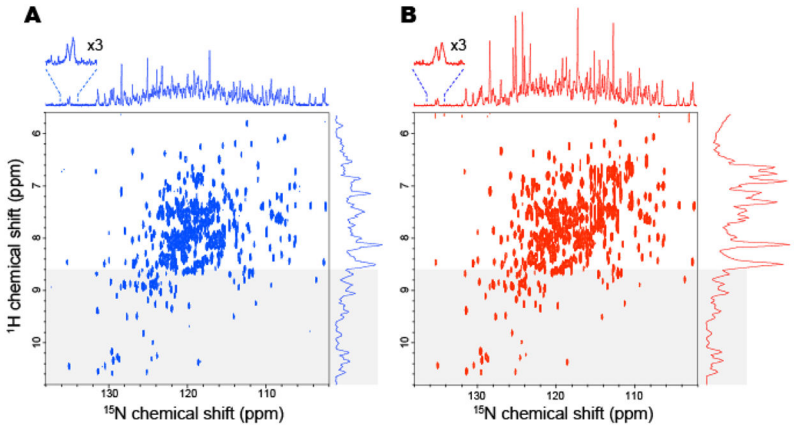

Figure 4. Comparison of (A) the ^{15}N-detected TROSY-HSQC and (B) the ^{1}H-detected TROSY-HSQC of 0.5 mM non-deuterated MBP in complex with 2 mM βCD at 283 K

(A) The ^{15}N-detected TROSY-HSQC was recorded in 8.5 hr, ns=176, F1=128 pts (14 ms), F2 = 2048 pts (315 ms). (B) The ^{1}H-detected TROSY-HSQC was recorded in 8.5 hr, ns = 12, F1= 2048 pts (315 ms), F2=800 pts (18 ms). The ^{1}H-detected TROSY-HSQC was transposed. ^{15}N and ^{1}H projections of the 2D spectra are indicated without any multiplication. The regions that were expected to contain mainly the resonances from the structured region of the proteins (> 8.6 ppm in ^{1}H dimension) are indicated by shadowing. The spectra were recorded at 283 K and 800 MHz, and the apparent τ_c of the system deduced from the TROSY for rotational correlation times (TRACT) experiment was 35 ns (Lee et al., 2006).